JOURNAL OF SOLID STATE CHEMISTRY 52, 114–123 (1984)

The Cubo-Octahedral Cluster in the Fluorite-Type Lattice: A Theoretical Approach

S. F. MATAR, J. M. REAU, AND P. HAGENMULLER

Laboratoire de Chimie du Solide du CNRS 351, cours de la Libération, 33405 Talence Cedex, France

AND C. R. A. CATLOW

Department of Chemistry, University College London, 20 Gordon Street, London WC1 H OAJ, U.K.

Received October 11, 1983

A cubo-octahedral cluster within the anionic sublattice is proposed as an extended defect in the AM_3F_{10} phases (A = K, Rb; M = Y, Bi). A computer simulation technique is used starting from crystallographic data to determine their validity and to evaluate some physical properties. A simulation study of new point defects in alkaline-earth fluorides doped with tetravalent cations is developed. The cubo-octahedral cluster is shown to be stable when it is introduced within the fluorite lattice. A mechanism is proposed for its formation on the basis of the aggregation of simpler defects.

I. The AM_3F_{10} Phases (A = K, Rb; M = Y, Bi)

1. Introduction

The fluorite-type structure (CaF_2) is well known for its ability to accommodate a large number of interstitial anions when the divalent cation is substituted by a tri- or tetravalent one (*1–4*). This structure is actually adopted by a certain number of compounds in which the cationic site is occupied by monovalent and trivalent ions, namely the $ABiF_4$ (A = K, Rb, Tl) phases which adopt the CaF_2-type structure at high temperature (*5*). Just like alkaline-earth fluorides, $ABiF_4$ phases can accommodate supernumerary fluorine ions leading to disordered solid solutions of formula $A_{1-x}Bi_xF_{1+2x}$ as well as to ordered ABi_3F_{10} phases (*6, 7*). A structure has been proposed for these phases (KY_3F_{10}-type structure) (*8*).

KY_3F_{10} crystallizes in the $Fm3m$ space group with Z = 8; 1:3 ordering is established between K^+ and Y^{3+}. It is characterized by the repetition in the three space directions of $[KY_3F_8]^{2+}$ and $[KY_3F_{12}]^{2-}$ groups. Whereas the "F_8" motifs are cubic the "F_{12}" motifs form a cubo-octahedral cluster (Fig. 1).

The aim of this work is to study the stability of the cubo-octahedron as an extended defect in the AM_3F_{10} phases. We examine this problem using theoretical simulations. The computer codes that have been used are PLUTO for the perfect lattice and CASCADE for the defect lattice

0022-4596/84 $3.00

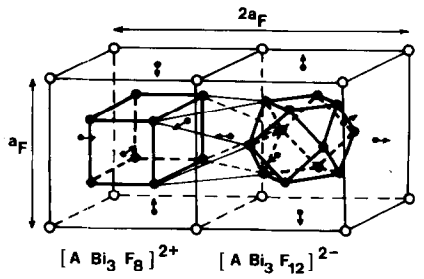

FIG. 1. Association of a fluorite-type and of a cubo-octahedral clusters of the anions in the KY_3F_{10} phases. •, Bi; ○, A(K, Rb); ●, F.

(see section II) (*9*). The formalism of these programs is discussed on the basis of the Born–Von Kàrmàn theory of the ionic crystal (*10*) and by Lidiard and Norgett (*11*).

In a material of largely ionic character the prevailing contribution to the cohesive energy is of the Coulomb-type. It can be considered as resulting from the interaction between charged and physically distinct ions. In a first approximation, all other interactions can be represented by short-range potentials acting between adjacent pairs of ions. Thus, the lattice cohesive energy per unit cell is

$$U = \tfrac{1}{2} \sum_{i,j} \frac{q_i q_j}{r_{ij}} + \tfrac{1}{2} \sum_{i,j} V(r_{ij}) \qquad (i \neq j)$$

where $V(r_{ij})$ is a short-range potential and r_{ij} the interionic separation between i and j ions.

It is well known that the calculation of the electrostatic component of the lattice energy involves the evaluation of the Madelung constant. Direct summations over the positive and negative ions can only yield an oscillating series whose terms decrease extremely slowly. This leads to numerical problems. In the computer codes used in this study, Coulomb sums are evaluated using the Ewald method (*12*) in which rapid convergence is assured by a transformation to reciprocal space.

The computer codes used combine accurate calculations of lattice energies with efficient minimization procedures to generate the lowest energy configuration of a proposed structure. A number of closely related computer codes are available for such works (PLUTO, METAPOCS, CASCADE); their methodology is discussed in detail in Ref. (*9*). As noted the PLUTO and CASCADE codes were used in the present study.

2. Microscopic Models for Ionic Representation

Two principal models are used to describe ionic properties in current simulation codes. These are as follows:

A. The Rigid Ion Model

This model assumes the particles to bear the full ionic charges (*14*). Ion polarizability is ignored. The optical dielectric constant is $\varepsilon_\infty = 1.0$. The static dielectric constant can be fitted to the experimental value by using a short-range interionic potential of the Born–Mayer-type (*10*):

$$V(r_{ij}) = A \exp(-r_{ij}/\rho) - C/r_{ij}^6$$

where A, ρ, and C are, respectively, a pre-exponential overlap repulsive term, a hardness factor, and a van der Waals constant for induced dipole–dipole attractions. The approximation of the Rigid Ion is very helpful when the calculation requires the simulation to be achieved by successive steps. This is actually the case in the Molecular Dynamics calculations (*15*) which are highly demanding in computer time.

B. The Shell Model

This model, first introduced by Dick and Overhauser (*16*) and further developed by Axe (*17*) and Cowley (*18*) accounts for ionic polarizability through a mechanical model. The ionic charge is shared between a core (the nucleus plus internal electrons) $X(e)$ and a spherical nondeformable shell (external electrons) $Y(e)$, so that $(X + Y)(e) = Z(e)$. The shell is bound to the core by a

TABLE I

SHORT RANGE AND SHELL MODEL POTENTIAL PARAMETERS USED FOR AM_3F_{10} (A = K, Rb; M = Y, Bi)

Pairs of ions	A (eV)	ρ (Å)	C (eV · Å^{-6})	k (eV · Å^{-2})	$Y(e)$
K^+–F^-	1,958.80	0.2865	0.0	86,032.0	− 85.55
Rb^+–F^-	961.00	0.3334	0.0	121,460.0	−125.30
Y^{3+}–F^-	1,635.60	0.3023	0.0	105.50	6.58
Bi^{3+}–F^-	721.13	0.3580	0.0	105.50	6.58
F^-–F^-	1,127.70	0.2753	26.8	37.98	− 1.339

spring of constant k. If b is the relative displacement of the shell with respect to the core, the potential for self-interactions within a given ion is

$$V(b) = \tfrac{1}{2}kb^2$$

This potential is harmonic. It acts in addition to the short-range potential. The polarizability α is proportional to $(Y(e))^2/k$.

We shall be mainly concerned in this work with the Shell model.

Both short-range potential and Shell-model potential parameters, i.e., C, k, and Y, can be fitted to the lattice properties of the crystal: lattice formation energy, elastic and dielectric constants using adaptations of the PLUTO code (*9*).

The preexponential repulsive factor A and the hardness factor ρ, can be obtained for specific interactions between isolated ions of opposite or identical charges using the nonempirical "electron-gas" method (*19*) which treats the electron density as a degenerate Fermi-gas.

The values of the parameters used in our investigations on the AM_3F_{10} phases are listed in Table I.

3. THE ORDERED PHASES: KY_3F_{10}, KBi_3F_{10}, AND $RbBi_3F_{10}$

In all three cases, the minimization procedure was started from the structural parameters reported by Pierce and Hong (*8*). The method uses iterative cycles requiring zero internal strains (zero force on each ion), at the end of the calculation, although the unit cell dimensions are held fixed. A relaxed structure results with new atomic positions and minimum energy.

Table IIA shows the results of the relaxation for the three phases. The following observations arise upon examining the results:

(a) The starting atomic positions (*8*) are in good agreement with those obtained after relaxation of the structure;

(b) The average value of the F'_{II} (48*i*) coordinates (0.50, 0.34, 0.34) is confirmed by the neutron diffraction investigation of the fluorite-type solid solutions $A_{1-x}Bi_xF_{1+2x}$ (A = K, Rb) (*20*) for the interstitial anions. This suggests the formation of cubo-octahedral "precursors" in the apparently disordered solid solution domain (see section II);

(c) The anionic sublattices (32*f*) and (48*i*) are affected by relaxation. Such a result is to be expected for this class of materials which are fluorine fast ionic conductors (*6*), although we are merely concerned here with static calculations.

Table IIB gives the calculated physical constants (i.e., lattice formation energy, elastic constants and dielectric constants) for the ordered phases. The zero internal strains obtained with the relaxed coordinates (Table IIA) employing the parameters presented in Table I suggest that the calculated physical properties will be reliable. Such physical properties are probably difficult to evaluate experimentally, due to diffi-

TABLE II

A. ATOMIC POSITIONS IN AM_3F_{10} PHASES BEFORE AND AFTER RELAXATION

Atom		Before relaxation (Ref. (*11*))	After relaxation		
			KY_3F_{10}	KBi_3F_{10}	$RbBi_3F_{10}$
M(K, Rb)	(8*c*)	$(\frac{1}{4},\frac{1}{4},\frac{1}{4})$ $(\frac{3}{4},\frac{3}{4},\frac{3}{4})$	$(\frac{1}{4},\frac{1}{4},\frac{1}{4})$ $(\frac{3}{4},\frac{3}{4},\frac{3}{4})$	$(\frac{1}{4},\frac{1}{4},\frac{1}{4})$ $(\frac{3}{4},\frac{3}{4},\frac{3}{4})$	$(\frac{1}{4},\frac{1}{4},\frac{1}{4})$ $(\frac{3}{4},\frac{3}{4},\frac{3}{4})$
N(Y, Bi)	(24*e*)	$(x,0,0)$; $x = 0.2401$	$x = 0.2388$	$x = 0.2402$	$x = 0.2403$
F_{II}	(32*f*)	(v,v,v); $v = 0.1081$	$v = 0.1095$	$v = 0.1110$	$v = 0.1095$
F'_{II}	(48*i*)	$(\frac{1}{2},u,u)$; $u = 0.3353$	$u = 0.3395$	$u = 0.3399$	$u = 0.3408$

B. CALCULATED PHYSICAL CONSTANTS FOR THE AM_3F_{10} PHASES

Material	Cohesive energy, U_L (eV)[a]	Elastic constants (10^{11} dyne · cm^{-2})			Dielectric constants		Bulk-lattice strains
		C_{11}	C_{12}	C_{44}	ε_s	ε_∞	
KY_3F_{10}	−41.57	14.54	6.30	5.66	8.705	3.53	0.005
KBi_3F_{10}	−39.31	11.69	5.44	4.55	11.690	3.48	−0.009
$RbBi_3F_{10}$	−39.16	11.28	5.09	4.26	10.714	3.48	−0.002

[a] Constant volume energies calculated per cation.

culties in obtaining adequate single crystals. This illustrates one of the important aspects of computer simulation of solids.

Finally, the values of U (eV) obtained for the three ordered phases are clearly reasonable when compared with the corresponding ordered AEF_2 fluorides (AE = Ca, Sr, Ba): $U_{CaF_2} = -26.76$ eV, $U_{SrF_2} = -25.33$ eV, $U_{BaF_2} = -23.81$ eV (*21*).

4. CONCLUSIONS

The calculations summarized in this section clearly confirm the stability of the cubo-octahedral cluster as a building block in ordered anion-excess fluorite phases. They show, moreover, that our computational methods can accurately reproduce the structure of these phases. This encourages confidence in the use of the methods for the more subtle structural problems posed by the related disordered systems.

II. A New Point Defect in Alkaline-Earth Fluorides Doped with Tetravalent Cations

1. INTRODUCTION

The physical properties of defective anion-excess fluorides with fluorite-type structures have been subject to exhaustive studies (*25–27*). Structural (*28*) and fundamental (*29*) aspects of the defects occuring for very low dopant concentrations within the alkaline-earth fluoride matrix (<1%) are now well understood (*23*). For instance, the pair defects "*nn*" (nearest neighbor) and "*nnn*" (next nearest neighbor) (Figs. 2a and b) are well established from EPR studies (*30*) and theoretical calculations (*29*). However, for high rates of dopant concentrations (>15%), the models proposed to account for clustering of point defects (*31*) are far less definite.

Therefore it seemed worthwhile to inves-

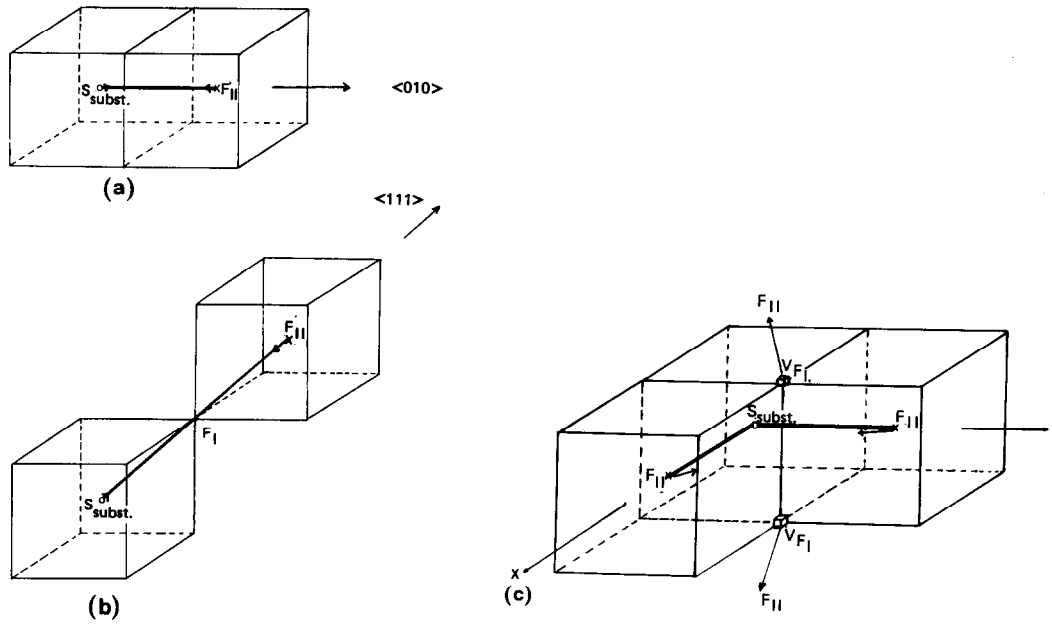

FIG. 2. Structures of the pair defects.

tigate new defect models consistent with any domain of concentration. On the other hand, we have previously shown (section I) that cubo-octahedral complex defects yield a stable configuration in AM_3F_{10} phases (A = K, Rb; M = Y, Bi).

Specifically we will perform calculations for the U^{4+}/CaF_2 solid solution using the potential parameters for this system reported in Table III.

2. Treatment of the Defective Lattice

The response of a perfect lattice to the introduction of a defect can be visualized through relaxations of the ions in order to adopt a new stable configuration, with a minimum of energy. These relaxations affect most directly the defect itself and a small region surrounding it. They decrease fairly rapidly for distances away from the defect. Thus it is convenient to partition the crystal into an inner Region I in which the lattice configuration is evaluated explicitly and an outer Region II which can be viewed *from the defect* as a dielectric continuum. The defect formation energy can be evaluated from the difference between the energy of the final configuration and that of the perfect lattice

Automated computer codes (HADES III, CASCADE) are available for such defect calculations. Their reliability is demonstrated in a large number of studies of ionic materials (*9*). The CASCADE code was used in the present study.

TABLE III

SHORT RANGE AND SHELL MODEL POTENTIAL PARAMETERS USED FOR $CaF_2(U^{4+})$

Ion pairs	A (eV)	ρ (Å)	C (eV · Å^{-6})	K(eV · Å^{-2})	$Y(e)$	Ref.
Ca^{2+}–F^-	1329.6	0.2979	0.0	390.90	5.24	(*34*)
U^{4+}–F^-	1755.6	0.3304	0.0	103.38	6.64	(*24*)
F^-–F^-	1127.7	0.2753	19.65	101.2	−2.38	(*35*)

TABLE IV

A. FORMATION ENERGIES (eV) OF ISOLATED DEFECTS AT CONSTANT VOLUME

	Defect				
	Anion vacancy	Anion interstitial	Anion Frenkel pair	Cation vacancy	U^{4+} subst.
Formation energy	5.76	−3.12	2.64	23.60	−44.19

B. DEFECT PAIR FORMATION AND BINDING ENERGIES (eV) PER SUBSTITUTIONAL CATION IN CaF_2: U^{4+} AT CONSTANT VOLUME

	Defect				
	nn pair ⟨100⟩	*nnn* pair ⟨111⟩	Angular dimer *nn*nn*	Angular dimer *nn*nnn*	1:3:1 trimer
Formation energy	−48.69	−48.09	−53.77	−52.45	−53.61
Binding energy	− 1.39	− 0.79	− 3.35	− 2.02	− 5.82

3. POINT AND PAIR DEFECTS

We have primarily considered the point defects (anion vacancy, anion interstitial, cation vacancy, U^{4+} substituent) and the pair defects *nn* and *nnn*. The results of the calculations are given in Table IV. The following observations arise upon their analysis:

The nearest-neighbor pair *nn* is energetically favored with regard to the next-nearest-neighbor pair *nnn*. On the other hand, we have calculated the formation energy of the angular dimer formed by the association of two interstitials (*nn*, *nn*) and (*nn*, *nnn*) (Table IV). The angular dimers are more stable than the elementary pairs and the (*nn*, *nn*) dimer is favored in comparison to the (*nn*, *nnn*) dimer. The structure of the (*nn*, *nn*) defect is shown in Fig. 2c before and after relaxation (which is indicated by arrows). This leads us to a more detailed study of the angular dimer.

The replacement of Ca^{2+} by U^{4+} involves the introduction of two fluorine ions in interstitial sites. The relaxation of such a configuration leads to an attraction of the interstitials by the substitutional cations and to the shift of two F^- at normal positions (on both sides of the plane formed by the dimer) into interstitial positions (Fig. 2c). Such a behavior corresponds to the substitution mechanism proposed in the neutron diffraction studies of the fluorite-type solid solution $Pb_{1-x}Th_xF_{2+2x}$ (*32*).

The relaxation of the angular dimer leads to strong relaxations within the anion sublattice around the defect. Such a disordering is probably favorable for enhanced ionic motion.

4. THE 1:3:1 TRIMER

Examination of the angular dimer within the unit cell before and after relaxation leads to several important features:

Before relaxation the immediate surrounding of U^{4+} is formed of two interstitials (F'_{II}) explicitly introduced and one fluoride ion $(F'_I)_A$ occupying a normal site. They may be differentiated by their positions and consequently their distances to the substitutional cation (Table VA).

TABLE V

A. BOND DISTANCES AND ANGLES IN THE ANGULAR DIMER *nn*nn*

	Before relaxation	After relaxation
$d_{U_{Ca}}$–2(F'_{II}) (Å)	2.725	2.329
$d_{U_{Ca}}$–$(F_I)_A$ (Å)	2.360	2.323
(F'_{II})–U–(F'_{II}) angle	90°	72.0°
$(F_I)_A$–U–(F'_{II}) angle	54.73°	68.6°
$d_{U_{Ca}}$–V_{F_I} (Å)	—	2.36

B. BOND DISTANCES AND ANGLES IN THE 1 : 3 : 1 TRIMER

	Before relaxation	After relaxation
$d_{U_{Ca}}$–3F'_{II} (Å)	2.725	2.319
$d_{U_{Ca}}$–V_{F_I} (Å)	2.360	2.360
$d_{U_{Ca}}$–U_{F_I} (Å)	90°	71.7°

After relaxation these three fluorine ions are nearly equivalent (Table VA), which is the consequence of a large shift of the above mentioned $(F_I^-)_A$ anion into an interstitial position with creation of a vacancy V_{F_I}. It is to be noticed that the other F_I^- anions are only slightly affected by relaxation phenomena.

The similar distances between U_{Ca} and the three relaxed F^- ions and the close values of the F-Û-F angles have led us to consider a new type of defect which will be called the 1 : 3 : 1 trimer (*nn*, *nn*, *nn*) involving, respectively, one U_{Ca}^{4+}, 3 equivalent F_{II}^- and $1V_{F_I}$ (Fig. 3). This configuration is electrically neutral.

We have simulated it by inserting interstitials at ideal lattice positions ($\frac{1}{2}$, 0, 0) and by creating a vacancy at normal position ($\frac{1}{4}$, $\frac{1}{4}$, $\frac{1}{4}$). Its relaxation yields a stable configuration very close to that of the relaxed angular dimer (Table VB).

The observation of both configurations, angular dimer and 1 : 3 : 1 trimer before and after relaxation, shows that the out-of-plane relaxations occur in the bisecting

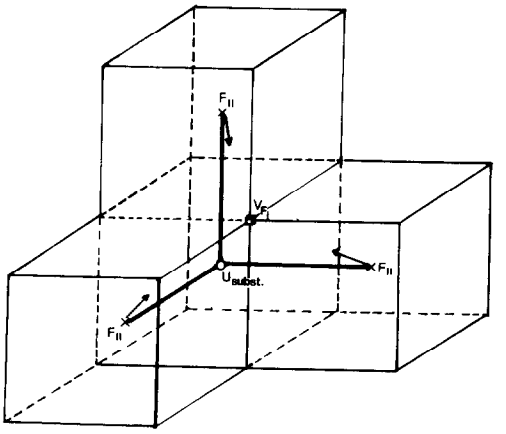

FIG. 3. The 1 : 3 : 1 trimer.

plane (110) (Fig. 4) and that the final positions in that plane (A_1 and B_1) together with the initial ones (A and B) form a sequence

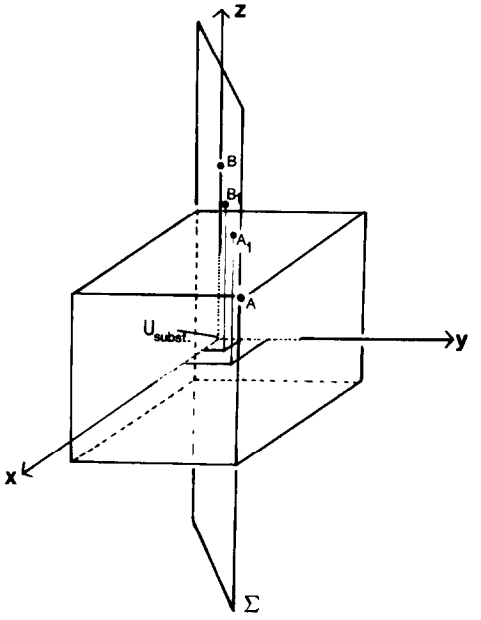

FIG. 4. Schematic correlation between the structures of the angular dimer and of the 1 : 3 : 1 trimer. Assignments of the F^- anions: A, F_I^- (0.25, 0.25, 0.25) angular dimer, unrelaxed; A_1, F_{II}^- (0.15, 0.15, 0.38) angular dimer, relaxed; B, F_{II}^- (0.0, 0.0, 0.5) 1 : 3 : 1 trimer, unrelaxed; B_1, F_{II}^- (0.09, 0.09, 0.44) 1 : 3 : 1 trimer, relaxed.

TABLE VI

A. BINDING ENERGY CALCULATION (CONSTANT VOLUME)

Formation energy of the defect: −446.0945 eV
Total binding energy = −446.0945 − (Energy of 8 anion vacancies
+ 12 Interstitial anions + 8 Substitutional cations)
= −446.0945 − (+ 8(5.76) − 12(3.12) − 8(44.19))
= −101.21 eV
Binding energy per substitutional cation = −12.65 eV

B. ATOMIC COORDINATES IN THE CUBO-OCTAHEDRAL CLUSTER

Species	Population	Coordinates before relaxation				Coordinates after relaxation			
U_{Ca}^{4+}	8	0.0	0.0	0.0	↻	−0.065	−0.065	−0.065	↻
V_{F_I}	8	0.25	0.25	0.25	↻	0.25	0.25	0.25	↻
F'_{II}	12	0.335	0.335	0.5	↻	0.360	0.360	0.5	↻
Ca_{Ca}	6	0.0	0.5	0.5	↻	0.111	0.5	0.5	↻

C. BOND DISTANCES (Å) IN THE CUBO-OCTAHEDRAL CLUSTER

	Before relaxation	After relaxation
$d_{U_{Ca}^{4+}-3F'_{II}}$	2.869	2.710
$d_{Ca_{Ca}-4F'_{II}}$	2.035	2.249
$d_{F_{II}-4F'_{II}}$	2.582	2.829
$V_{\text{cubo-octahedron}}$ (Å^3)	24.353	32.00

pointing out the close relationship between the dimer and the trimer.

The calculations of the formation and binding energies of the 1 : 3 : 1 trimer given in Table IVB show that it is favored with regard to all other defects so far studied. We can thus suggest that the formation of this new type of defect must follow immediately that of the angular dimer (*nn*, *nn*).

5. THE CUBO-OCTAHEDRAL CLUSTER

From the structure of the AM_3F_{10} phases which is closely related to the fluorite-type structure (CaF_2), it appears reasonable to suggest a complex defect likely to occur within CaF_2 itself: the cubo-octahedron.

Formally in CaF_2 the anionic sublattice is modified by creating 8 vacancies at normal sites and inserting 12 interstitials in the same manner as in KY_3F_{10} (see Part I). The relaxation of such a configuration leads to satisfactory convergence. However, the binding energy of a cluster where the cationic sublattice would not be modified is positive: the F_{12} cluster is not bound. On the contrary the relaxation of the effective $[Ca_3UF_{12}]^{2-}$ cluster (U^{4+} replacing Ca^{2+} at the fluorite-type cube corners) yields a valid minimization of the energy as well as a stable configuration. The binding energy of the defect is found to be −12.65 eV.

Table VIA shows the detailed calculation of the binding energy. We should state that this value is approximate, since the formation energy of a defect is sensitive to the radius chosen for Region I, i.e., the region where ionic interactions are evaluated explicitly (see Ref. *36*). With regard to the

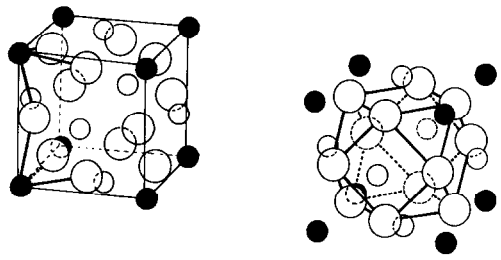

FIG. 5. Formation of the $[Ca_3UF_{12}]^{2-}$ cluster by association of 1 : 3 : 1 trimers. ○, F_{II}'; ○, Ca; ●, U_{Ca}.

large dimension of the cubo-octahedral defect a bigger radius may be preferable for Region I. Nevertheless the large difference between the binding energies of the cubo-octahedron on one hand (−12.65 eV) and the 1 : 3 : 1 trimer (−5.84 eV) suggests that the cluster will be stable.

Table VIB and C give the relaxed atomic coordinates and the interionic distances in $[Ca_3UF_{12}]^{2-}$. The relaxed F_{II}–$4F_{II}$ shortest distances (2.829 Å) are larger than in KY_3F_{10} where they are equal to 2.685 Å. This is probably due to the higher charge of the U^{4+} substitutional which attracts the interstitial anions. In fact the relaxation results in an expansion of the cubo-octahedron.

Needless to say that the $[Ca_3UF_{12}]^{2-}$ motif has to be electrically compensated by a $[Ca_3UF_8]^{2+}$ motif (Fig. 1).

The cubo-octahedral cluster has been successfully simulated as well in SrF_2 and BaF_2 doped with the tetravalent cations.

6. DISCUSSION

In former sections the investigation of the structure of the relaxed angular dimer has shown its direct relationship with the substitution mechanism proposed by neutron diffraction investigations (*9*). On another hand the stability of the 1 : 3 : 1 trimer with respect to the dimer has been proved.

An increasing amount of substitutionals in the structure of CaF_2 should thus lead to an increasing number of 1 : 3 : 1 trimers and further on to their clustering. This, we suggest, occurs through the formation of the cubo-octahedron by associating $8[U_{Ca}F_3V_F]$ defects, i.e., eight 1 : 3 : 1 trimers by sharing F_{II}' interstitials two by two. This result is illustrated in Fig. 5.

Such a mechanism needs a crystallographic support. Nevertheless the formation of the cubo-octahedron as a complex type of clustering seems to be well established. The assumption made by Pierce and Hong (Ref. (*8*)) that ". . . Such isolated subcells (cubo-octahedral motifs) in the fluorite-type lattice are bound to occur upon doping" is now demonstrated crystallographically by a recent investigation of the "Tveitite" mineral by Bevan *et al.* (*33*).

Following Bevan *et al.* we suggest that the formation of the cubo-octahedron is prior to the onset of ordering which can only be total when the number of cubo-octahedral motifs becomes sufficient. This is the case for the AM_3F_{10}-ordered phases.

Notes added in proof. (i) In a paper to be published shortly in this general area we show that the stability of cubo-octahedral motifs relative to that of smaller defect clusters depends on the radius of the dopant ion. (ii) The binding energy calculated in Table VI assumed preexisting vacancies. If it is assumed that these vacancies are created during the formation of the cluster, the binding energy per cation is reduced to 10.01 eV.

References

1. O. VON GREIS AND M. KIESER, *Z. Anorg. Allg. Chem.* **479,** 165 (1981).
2. B. P. SOBOLEV, K. B. SEIRANIAN, AND L. S. GARASHINA, *J. Solid State Chem.* **28,** 51 (1979).
3. I. D. RATNIKOVA, YU. M. KORENEV, B. P. SOBOLEV, AND A. V. NOVOSELOVA, *Proc. Moscow Univ., Chem.* N°2 (1977).
4. J. P. LAVAL, B. FRIT, AND B. GAUDREAU, *Rev. Chim. Miner.* **16,** 509 (1979).
5. C. LUCAT, PH. SORBE, J. PORTIER, J. M. RÉAU, AND P. HAGENMULLER, *Mater. Res. Bull.* **12,** 145 (1977).
6. S. MATAR, J. M. RÉAU, C. LUCAT, J. GRANNEC, AND P. HAGENMULLER, *Mater. Res. Bull.* **15,** 1295 (1980).

7. S. MATAR AND J. M. RÉAU, *C.R. Acad. Sci. II* **294,** 649 (1982).
8. J. W. PIERCE AND H. Y. P. HONG, *Proc. Rare Earth Res. Conf. 10th,* Carefree, Arizona, A2, 527 (1973).
9. C. R. A. CATLOW AND W. C. MACKRODT, Eds., *in* "Computer Simulation of Solids," Chap. I, Springer-Verlag, Berlin/Heidelberg/New York (1982).
10. M. BORN AND K. HUANG, "Dynamical Theory of Crystal Lattices," Oxford Univ. Press (Clarendon), London/New York (1962).
11. A. B. LIDIARD AND M. J. NORGETT, *in* "Computational Solid State Physics" (F. Herman, N. W. Dalton, and T. R. Kohler, Eds.), p. 385, Plenum, New York (1972).
12. M. TOSI, *Solid State Phys.* **16,** 1 (1962).
13. B. SZIGETTI, *Proc. Roy Soc. Sect. A* **204,** 51 (1950).
14. R. SRINIVASAN, *Phys. Rev.* **165,** 3, 1054 (1968).
15. A. B. WALKER, M. DIXON, AND M. J. GILLAN, *Solid State Ionics* **5,** 601 (1981).
16. B. G. DICK, AND A. W. OVERHAUSER, *Phys. Rev.* **112,** 90 (1958).
17. J. D. AXE, *Phys. Rev. A* **139,** 1215 (1965).
18. R. A. COWLEY, *Proc. Roy. Soc. London A* **268,** 109 (1962).
19. R. G. GORDON AND Y. S. KIM, *J. Chem. Phys.* **56,** N°6 (1972).
20. J. L. SOUBEYROUX, J. M. RÉAU, S. MATAR, G. VILLENEUVE, AND P. HAGENMULLER, *Solid State Ionics* **6,** 103 (1982).
21. J. D. AXE, J. W. GAGLIANELLO, AND J. SCARDEFIELD, *Phys. Rev.* **139,** N° 4A, 1211 (1965).
22. C. R. A. CATLOW, K. M. DILLER, AND M. J. NORGETT, *J. Phys. C.* **10,** 1935 (1977).
23. J. CORISH, C. R. A. CATLOW, P. W. M. JACOBS, AND S. H. ONG, *Phys. Rev. B* **25,** 6425 (1982).
24. A. N. CORMACK, private communication.
25. J. M. RÉAU, AND J. PORTIER, *in* "Solid Electrolytes" (P. Hagenmuller and W. Van Gool, Ed.), Chap. 19, Academic Press, New York (1978).
26. K. E. WAPENAAR AND J. SCHOONMAN, *J. Electrochem. Soc.* **126,** N°4, 667 (1979).
27. H. W. HARTOG AND J. C. LANCEVOORT, *Phys. Rev. B* **24,** N°6, 3547 (1981).
28. A. K. CHEETHAM, B. E. F. FENDER, D. STEELE, R. I. TAYLOR, AND B. I. M. WILLIS, *Solid State Commun.* **8,** 171 (1970).
29. C. R. A. CATLOW, *J. Phys. C.* **9,** 1845 (1976).
30. E. L. KITTS, M. IKEYA, AND J. H. CRAWFORD, *Phys. Rev. B* **8,** 5840 (1973).
31. A. K. CHEETHAM, B. E. F. FENDER, AND M. J. COOPER, *J. Phys. C* **4,** 3107 (1971).
32. J. L. SOUBEYROUX, J. M. RÉAU, S. MATAR, P. HAGENMULLER, AND C. LUCAT, *Solid State Ionics* **2,** 215 (1981).
33. D. J. M. BEVAN, J. STRÄHLE, AND O. GREIS, *J. Solid State Chem.* **44,** 75 (1982).
34. C. R. A. CATLOW, Ph.D. thesis, University of Oxford (1974).
35. C. R. A. CATLOW, M. J. NORGETT, T. A. ROSS, Harwell Report T. P. 673 (1976).
36. M. J. NORGETT, A. E. R. E. HARWELL Report N° 7650 (1974).